Airway epithelial cell differentiation relies on deficient Hedgehog signalling in COPD

Randa Belgacemi, Emilie Luczka, Julien Ancel, Zania Diabasana, Jeanne-Marie Perotin, Adeline Germain, Nathalie Lalun, Philippe L. Birembaut, Xavier Dubernard, Jean-Claude Mérol, et al.

EBioMedicine 51 (2020) 102572

Contents lists available at ScienceDirect

EBioMedicine

journal homepage: www.elsevier.com/locate/ebiom

Research paper

Airway epithelial cell differentiation relies on deficient Hedgehog signalling in COPD

Randa Belgacemi[a], Emilie Luczka[a], Julien Ancel[a,b], Zania Diabasana[a], Jeanne-Marie Perotin[a,b], Adeline Germain[a], Nathalie Lalun[a], Philippe Birembaut[a,c], Xavier Dubernard[d], Jean-Claude Mérol[a,d], Gonzague Delepine[a,e], Myriam Polette[a,c], Gaëtan Deslée[a,b], Valérian Dormoy[a,*]

[a] Université de Reims Champagne-Ardenne, INSERM, P3Cell UMR-S1250, SFR CAP-SANTE, Reims 51097, France
[b] CHU Reims, Hôpital Maison Blanche, Service de pneumologie, Reims 51092, France
[c] CHU Reims, Hôpital Maison Blanche, Laboratoire de biopathologie, Reims 51092, France
[d] CHU Reims, Hôpital Robert Debré, Service d'oto-rhino-laryngologie, Reims 51092, France
[e] CHU Reims, Hôpital Robert Debré, Service de chirurgie cardio-vasculaire et thoracique, Reims 51092, France

ARTICLE INFO

Article History:
Received 3 September 2019
Revised 11 October 2019
Accepted 20 November 2019
Available online 23 December 2019

Keywords:
Chronic obstructive pulmonary disease
Airway epithelial cells
Differentiation
Cilia
Hedgehog

ABSTRACT

Background: Hedgehog (HH) pathway is constantly under scrutiny in the context of organ development. Lung morphogenesis requires HH signalling which participates thereafter to the pulmonary homeostasis by regulating epithelial cell quiescence and repair. Since epithelial remodelling is a hallmark of Chronic Obstructive Pulmonary Disease (COPD), we investigated whether the main molecular actors of HH pathway participate to airway epithelial cell differentiation and we analysed their alterations in COPD patients.
Methods: Sonic HH (Shh) secretion was assessed by ELISA in airway epithelial cell (AEC) air-liquid interface culture supernatants. HH pathway activation was evaluated by RT-qPCR, western blot and immunostaining. Inhibition of HH signalling was achieved upon Shh chelation during epithelial cell differentiation. HH pathway core components localization was investigated in lung tissues from non-COPD and COPD patients.
Findings: We demonstrate that progenitors of AEC produced Shh responsible for the activation of HH signalling during the process of differentiation. Preventing the ligand-induced HH activation led to the establishment of a remodelled epithelium with increased number of basal cells and reduced ciliogenesis. Gli2 activating transcription factor was demonstrated as a key-element in the regulation of AEC differentiation. More importantly, Gli2 and Smo were lost in AEC from COPD patients.
Interpretation: Our data suggest that HH pathway is crucial for airway epithelial cell differentiation and highlight its role in COPD-associated epithelial remodelling.

1. Introduction

Chronic obstructive pulmonary disease (COPD) is the fourth leading cause of death worldwide and affect the daily lives of millions [1,2]. If the main risk factors are clearly identified [3], characterization of various clinical phenotypes, early detection of the disease and identification of therapeutic approaches represent critical challenges to alleviate its socio-economic burden [4–8].

Cellular and molecular mechanisms responsible for the development and progression of COPD are not fully understood. The alteration of epithelial plasticity is one of the hallmark of the two main features observed in COPD patients: airway obstruction and emphysema [9–11]. Understanding the origin of epithelial remodelling is therefore crucial to propose novel biomarkers and elaborate innovative therapeutics. So far, dysregulation of basal cell differentiation, motile cilia defects and secretory cells dysfunctions have been reported and characterized [12,13], but no association was demonstrated between altered molecular events and cell fate except for BMP signalling [14].

Recent evidence indicate that some actors of HH pathway are present in adult lung epithelia and may play a role in respiratory diseases [15–17]. Canonical HH signalling refers to the activation of the pathway via binding of the ligand (Shh, Dhh or Ihh) to its receptor Ptch to release Smo receptor and relay Gli family transcription factors activity. Non-canonical HH signalling includes three modalities: (i) ligand-dependent/Smo-independent activation; (ii) ligand-dependent/Gli-independent

* Corresponding author at: Inserm UMR-S 1250, University of Reims Champagne-Ardenne, CHU Maison Blanche, 45 rue Cognacq-Jay, Reims 51092, France.
E-mail address: valerian.dormoy@univ-reims.fr (V. Dormoy).

https://doi.org/10.1016/j.ebiom.2019.11.033

Research in context

Evidence before this study

Hedgehog signalling is essential during lung development and it has been associated with COPD pathogenesis in GWAS. In addition, it was recently shown that components of Hedgehog pathway were present in lung ciliated cells and the receptor Ptch1 was found altered in COPD airway epithelia. However, it is not known how the core components of Hedgehog pathway take part in airway epithelial cell fate determinism and what the level of activation in COPD patients is.

Added value of this study

This is the first study to analyse all the five core components of Hedgehog pathway activation during airway epithelial cell differentiation *in vitro* and in the airways of patients. We identified the cells producing the ligand Sonic Hedgehog and we demonstrated that Hedgehog pathway activation is necessary for the establishment of a fully functional epithelium. We observed that the transcription factor Gli2 was partially responsible for the lack of ciliogenesis upon Hedgehog pathway inhibition. Furthermore, we provided the first evidence of Gli2 and the receptor Smo as key markers in COPD pathogenesis.

Implications of all available evidence

There is now accumulating evidence that Hedgehog pathway is involved in respiratory diseases.

Our findings suggest possibilities of making use of Hedgehog pathway elements as COPD markers as well as potential targets to manipulate airway epithelial cell differentiation.

Further studies are warranted to fully characterize the mechanisms associating Hedgehog pathway activation and epithelial cell fate or remodelling in respiratory dysfunctions.

activation; (iii) Gli-only activation [18–21]. Thus, HH signalling is required in early and postnatal lung development [15,22,23] and orchestrates adult lung repair and regeneration [24,25]. In addition, genome-wide association studies performed in COPD and non-COPD patients identified genetic alterations of HH-linked molecular actors [26–28]. Furthermore, HH signalling elements were recently observed in adult airways motile cilia [29] while Ptch1 was found to be associated with an increase of mucus production in severe COPD patients [30]. To date, the activation of the signalling cascade has not been linked to AEC differentiation and epithelial remodelling as seen in chronic lung disease pathology. Here we hypothesize that HH signalling orientates cell fate during differentiation and its alteration participates to respiratory disease.

We report that progenitors of airway epithelial cells produced Shh ligand to activate HH signalling during the course of differentiation *in vitro*. Aiming to suppress canonical and non-canonical HH signalling, an antibody against Shh was used in air-liquid interface cultures. We characterized the involvement of Shh signalling via the transcription factor Gli2 in the determinism of basal cells towards ciliated cells. Finally, we identified crucial differential localizations of Gli2 and Smo in non-COPD and COPD bronchial epithelium unveiling a potential innovative biomarker.

2. Materials and methods

2.1. Human subjects

Patients scheduled for lung resection for cancer (University Hospital of Reims, France) were prospectively recruited (n = 40) following standards established and approved by the institutional review board of the University Hospital of Reims, France (IRB Reims-CHU 20110612). In addition, 20 patients who underwent a routine fiber-optic bronchoscopy with bronchial brushings under local anaesthesia according to international guidelines were also recruited [31]. Informed consent was obtained from all the patients. Patients with asthma, cystic fibrosis, bronchiectasis or pulmonary fibrosis were excluded. At inclusion, age, sex, smoking history, and pulmonary function tests results were recorded. Ex-smokers were considered for a withdrawal longer than 6 months. COPD was defined by post-bronchodilator $FEV_1/FVC < 70\%$ [32]. The severity of COPD was determined by spirometric classification (GOLD 1: $FEV_1 \geq 80\%$ predicted, GOLD 2: $50\% \leq FEV_1 < 80\%$ predicted, GOLD 3: $30\% \leq FEV_1 < 50\%$ predicted, GOLD 4: $FEV_1 < 30\%$ predicted).

2.2. Human primary airway epithelial cell cultures

Human primary airway epithelial cells (AEC) were obtained from nasal polyps resected from non-COPD patients (11 donors) at the University Hospital of Reims to establish air-liquid interface (ALI) cultures as described by us and others [33–38]. Cells were dissociated by overnight pronase incubation (0.5 mg/mL, Sigma-Aldrich) and counted with ADAM (NanoEnTek) according to NanoEnTek instructions. 200,000 cells were seeded on 12-well plates containing 0.4 μm Transwells (Corning, Fisher Scientifc) coated with 0.3 mg/mL collagen type IV from human placenta (Sigma-Aldrich). PneumaCult-EX (PnC-Ex) media (StemCell) was used for initial proliferation in apical and basal chambers. Upon reaching cell confluency, the apical medium was removed and PneumaCult-ALI (PnC-ALI, StemCell) medium was used in basal chamber. Culture medium was changed three times a week and cells kept in incubators at 37 °C, 5% CO_2. Cells and supernatants were collected every 7 days to generate kinetic analysis. No heterogeneity was observed in terms of initiation of ALI (less than 10 days after seeding) and establishment of ciliogenesis (coverage of the apical surface with cilia above 75%). Inhibition of Sonic Hedgehog signalling was achieved upon AB5E1 (AB_2188307, Interchim, 1ug/ml, diluted in sterile water) addition to the culture medium as indicated in the following figures. Experimental design was extrapolated from pharmacological binding studies [39–43], as well as previously published reports resorting to AB5E1 in order to capture Shh [44–49]. Cell morphological changes were weekly evaluated under a microscope.

2.3. TEER measurements

Transepithelial electrical resistance (TEER) was evaluated at ALI-35 using an EVOM2 resistance meter with an STX2 electrode (World Precision Instruments Hitchin) at room temperature. The electrode was equilibrated in PnC-ALI during 1 h at room temperature before measurement. One mL PnC-ALI was added to the apical compartment and triplicate measurements were performed per sample. Data were corrected for blank values and area. Average resistance was subtracted from the measured value of every well according to data acquired on cell-free permeable supports and results are presented as resistance per surface (Ω x cm2).

2.4. RT-qPCR analyses

Total RNA from AEC (ALI cultures or bronchial brushings) was isolated by High Pure RNA isolation kit (Roche Diagnostics) and 250 ng were reverse-transcribed into cDNA by Transcriptor First Stand cDNA Synthesis kit (Roche Diagnostics). Quantitative PCR reactions were performed with fast Start Universal Probe Master kit and UPL-probe system in a LightCycler 480 Instrument (Roche Diagnostics) as recommended by the manufacturer. Specific primers (Eurogentec) were: SHH forward 5′-GCTTCGACTGGGTGTACTACG-3′,

reverse 5′- GCCACCGAGTTCTCTGCT-3′; GLI1 forward 5′- CCAGCCAGAGAGACCAACAG-3′, reverse 5′- CCCGCTTCTTGGTCAACTT-3′; GLI2 forward 5′- CTACCTCAACCCCGTGGAC-3′, reverse: 5′-CTGAGAGTGGGGAGATGGAC-3′; GLI3 forward 5′-ACATGGAATATCTTCATGCTATGG-3′, reverse 5′-GGTGATATGGACAGTGTACGTTTT-3′; CK5 forward 5′-TTCATGAAGATGTTCTTTGATGC-3′, reverse 5′-AGGTTGCGGTTGTTGTCC-3′; FOXJ1 forward 5′-CAGATCCCACCTGGCAGA-3′, reverse 5′-CGTACTGGGGGTCAATGC-3′, MUC5AC forward 5′-CACGTCCCCTTCAATATCCA-3′, reverse 5′-GGCCCAGGTCTCACCTTT-3′; MUC5B forward 5′-GTACAATGGCACCTTCTACGG-3′, reverse 5′-CTGACATTGCACCGTTGG-3′; SMO forward 5′-ATGGCACCATGAGGCTTG-3′, reverse 5′-GGGCGTAGTACACGATGACA-3′; PTCH1 forward 5′-GGCCTGGCAGAGGACATA-3′, reverse 5′- GGAAAGCACCTTTTGAGTGG-3′. Results for all expression data regarding transcripts were normalized to the expression of the house-keeping gene GAPDH amplified with the following primers: forward 5′-ACCAGGTGGTCTCCTCTGAC-3′, reverse 5′-TGCTGTAGCCAAATTCGTTG-3′. Relative gene expression was assessed by the ΔΔCt method [14] and expressed as fold change (log2, AB5E1 vs control) when indicated.

2.5. Immunofluorescent staining and analyses

Immunohistochemistry was performed on formalin-fixed paraffin-embedded (FFPE) lung tissues distant from the tumour as previously described [50] and frozen tissues. Five 5 μm sections were processed for H&E staining and observed on microscope (x20) to confirm the presence of bronchi. Bronchial epithelium was analysed on the entire slide including 2 to 7 bronchi per patient. FFPE lung tissues sections slides were deparaffinised and blocked with 10% BSA in PBS for 30 min at room temperature. Tissue sections were then incubated with the following primary antibodies for one night at 4 °C in 3% BSA in PBS: rabbit anti-Arl13b (17711−1-ap, ProteinTech, 1:200); mouse anti-Muc5ac (NBP2-15196, Novus Biologicals, 1:100); rabbit anti-Muc5B (E-AB-15988, Elabscience, 1:100); mouse anti-Acetylated-α-tubulin (T6793, Sigma Aldrich, 1:1000); goat anti-P63 (AF1916, R&D systems, 1:100); rabbit anti-Gli1 (HPA065172, Sigma Aldrich, 1 μg/mL); rabbit anti-Gli2 (HPA074275, Sigma Aldrich, 0,4 μg/mL); rabbit anti-Gli3 (HPA005534, Sigma, 0,6 μg/mL); goat anti-Shh (AF464, R&D Systems); rabbit anti-Smoothened (E-AB-12925, Elabscience, 1:50) and rabbit anti-Patched1 (E-AB-10571, Elabscience, 1:100). Sections were washed with PBS and incubated with the appropriate secondary antibodies in 3% BSA in PBS for 1 h at room temperature. DNA was stained with DAPI during incubation with the secondary antibodies. Micrographs were acquired by AxioImageur Zeiss (20x Ph) with ZEN software (8.1, 2012) and processed with ImageJ (National Institutes of Health) for analysis. For each patient, five random fields per section containing bronchi were taken to evaluate the localization of Gli2 and Smo on epithelial cells. Total epithelium length was measured by ImageJ and the presence of the protein of interest was assessed in 5 sub-compartments: cilia, sub-cilia, cytoplasm, cytoplasmic membrane, and nuclei.

2.6. Whole-mount immunofluorescent immunostaining

Methanol fixed AEC from ALI cultures were rehydrated by decreasing methanol concentration before a post fixation with acetone. Cells were then blocked with 10% BSA in PBS for 2 h at room temperature and incubated with previous primary antibodies for one night at 4 °C in 3% BSA in PBS. Cells were washed with PBS and incubated with the appropriate secondary antibodies in PBS for 2 h at room temperature. DNA was stained with DAPI during incubation with the secondary antibodies. Clarification of cells was achieving by a glycerol gradient (25%/50%/75%) before mounting the slides. Micrographs were acquired by Confocal Zeiss LSM710 microscope (20X/0.8) with ZEN software (8.1, 2012) and processed with ImageJ for max-intensity z-stack projections.

2.7. Immunoblot analyses

AEC were lysed on ice in RIPA (Radioimmunoprecipitation assay) buffer (50 mM Tris pH 7,4, 150 mM NaCl, 1% (v/v) Igepal, 1% (w/v) sodium deoxycholate, 5 mM iodoacetamide and 0,1% (v/v) SDS) supplemented with protease inhibitor cocktail inhibitor (Roche diagnostics), then lysates were clarified by centrifugation (13,000 × g for 10 min at 4 °C). Ten μg of total proteins quantified by Biorad DC protein Assay Reagent Package (Biorad) were submitted to electrophoresis. Subcellular Protein Fractionation Kit (Thermo Scientific) was used to resolve proteins according to their subcellular localizations following the manufacturer's instructions.

Primary antibodies were anti−Gli1 (AF3455, R&D Systems), anti-Gli2 (HPA074275, Sigma Aldrich), anti-Gli3 (HPA005534, Sigma Aldrich), anti-Patched1 (E-AB-10571, Elabscience), anti-Smoothened (NBP2-24543, Novus Biologicals), anti-Ck5 (AB24647, Abcam, Cambridge), anti-GAPDH (clone 6C5, Chemicon, Millipore), anti-Foxj1 (14−9965−82, Ebioscience, ThermoFisher Scientific). Membranes were incubated with appropriate dilutions of primary antibody followed by the appropriate peroxidase-conjugated secondary antibody (Bio-Rad Laboratories). Final detection was obtained by enhanced chemiluminescence (GE Healthcare). Detected signals were digitally compared using ImageJ.

2.8. Immunoprecipitation assays

Complexation of AB5E1 to Shh was evaluated by 24 h incubation of 2 mL of medium supplemented with different concentrations of mouse IgG1 negative control (clone 1E2.2, CBL610, Millipore) or AB5E1 at 37 °C, 5% CO2 and subsequent overnight incubation with G Sepharose proteins (P3296, Sigma Aldrich) at 4 °C. Immunocomplexes were isolated by series of centrifugation (13,000 × g for 10 min at 4 °C), washed with PBS, resolved by SDS-PAGE and transferred to PVDF membranes (PerkinElmer). Remaining steps were performed as described in immunoblot analyses.

2.9. ELISA

Concentrations of Shh proteins in apical and basal chambers supernatants (100 μL) were assayed by enzyme-linked immunosorbent assay (ELISA) according to the RayBiotech instructions (ELH-ShhN-001). The detection threshold for the assay was 8pg/mL.

2.10. Statistics

Quantitative variables were described with whisker plots as median ± interquartile range and clinical parameters were represented with dot plot and median. Qualitative variables were compared using Chi-square test or Fisher exact test as appropriate. Parametric tests were used after normal distributions and variance equality hypothesis verified respectively by Fisher's and Shapiro-Wilk tests. Quantitative data in multiple groups were analysed using repeated measures analysis of variance (ANOVA) following of a Tukey posthoc HSD test while two groups were compared with Student's test. If applications conditions were not filled, non-parametric Wilcoxon and Kruskal-Wallis tests were preferred. Linear regression was performed using Spearman test. In all exploratory analyses, results with two-sided p-value ≤ 0.05 were considered significant. The XLSTAT software (version 2019.1.3, Addinsoft company) was used to analyse and reformat data within Excel for statistical analysis and represented with GraphPad software Inc. Prism Version 8, US.

3. Results

3.1. Shh-Gli pathway is activated during airway epithelial cell differentiation

To determine whether HH pathway participated in the process of differentiation on airway epithelial cells (AEC), we investigated the potential activators of the molecular cascade. Interestingly, secreted Shh but not Dhh and Ihh was found in ALI medium (Fig. 1A). This ligand was also found in cell culture supernatants from AEC and in total protein extracts from human bronchi suggesting the production of Shh by AEC (Fig. 1A). In addition, we detected Shh by ELISA on the apical side of AEC ALI cultures at the start of differentiation (40.1 ± 46 pg/ml of supernatant after ALI switch) and predominantly on the basal side after fourteen days post-ALI (215±179 pg/ml, Fig. 1B–D). Immunostainings confirmed the presence of Shh preferentially in non-differentiated cells (Fig. 1E). Thus, basal AEC seemed responsible for Shh secretion.

We next investigated the core components of canonical HH activation on both transcripts and protein levels and localizations during the course of *in vitro* AEC differentiation. First, GLI2, GLI3, SMO and PTCH1 transcripts levels increased concomitantly with the

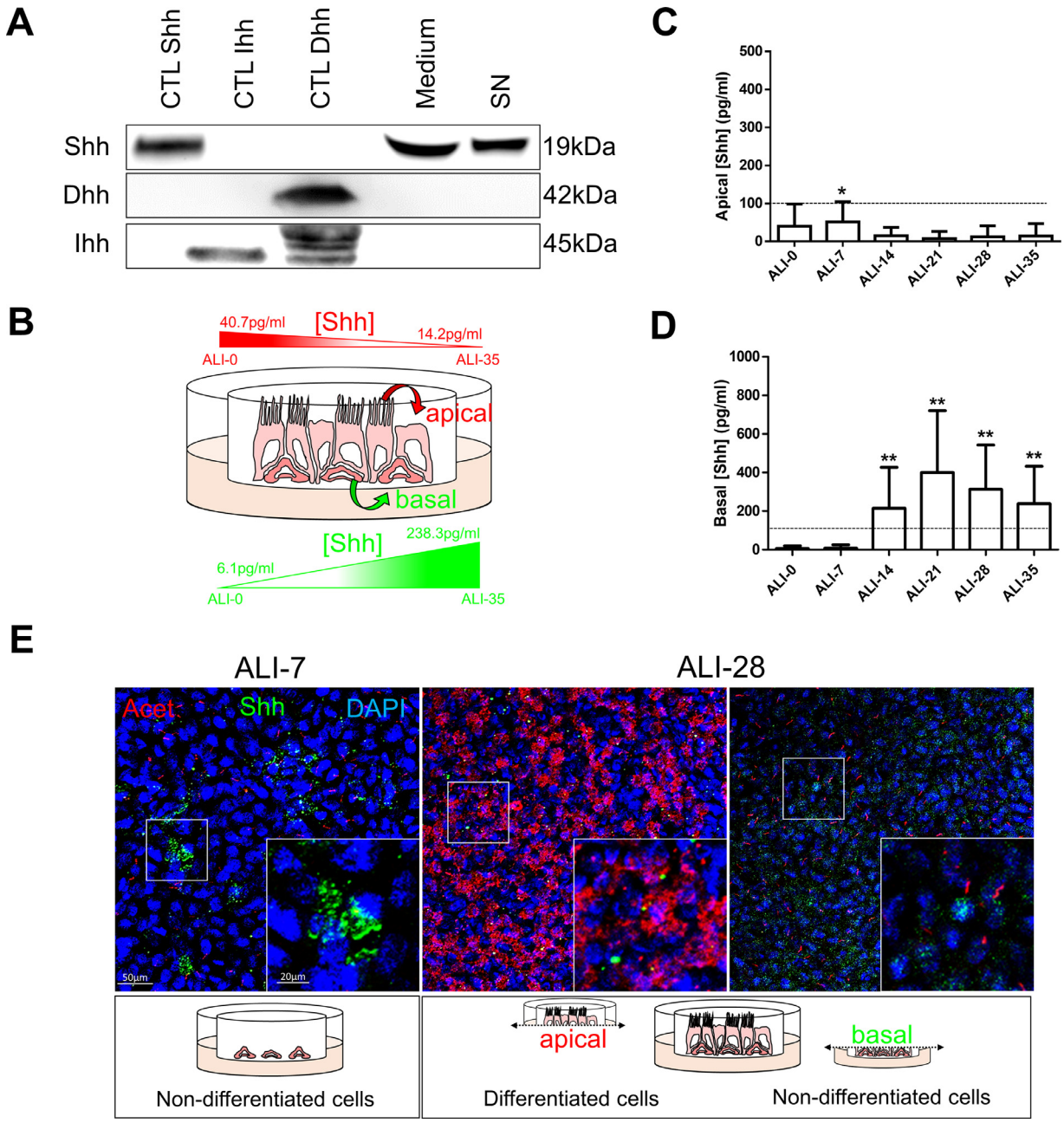

Fig. 1. Shh is produced by AEC. **A**, Representative immunoblots ($n = 3$) of Shh, Dhh and Ihh on human bronchi (CTL Shh), murine colon (CTL Ihh) and testis (CTL Dhh), AEC ALI culture medium (Medium), AEC ALI culture supernatants (SN). **B**, The schematic represents the gradients of Shh on AEC ALI cultures **C**, Histogram representing the concentration of Shh measured by ELISA in AEC cultures supernatants ($n = 11$) at the apical side during the process of differentiation (from ALI-0 to ALI-35). Results show mean ±SEM, $^{*}p < 0.05$ from reference value (8pg/ml). **D**, Histogram representing the concentration of Shh measured by ELISA in AEC cultures supernatants ($n = 11$) at the basal side during the process of differentiation (from ALI-0 to ALI-35). Results show mean ±SEM, $^{**}p < 0.01$ from reference value (8pg/ml). **E**, Representative confocal acquisitions from AEC cultures at ALI-7 and ALI-28 for Shh (green); cilia (acetylated tubulin, red) and cell nuclei (DAPI, blue). Merged z-projections are shown with a magnification corresponding to the selected area. Cartoons depict the cell differentiation status at the time of analysis. (For interpretation of the references to colour in this figure legend, the reader is referred to the web version of this article.)

differentiation of the epithelium (Fig. 2A) as detected by CK5 (non-differentiated cells marker), FOXJ1 (ciliated cells marker), MUC5AC and MUC5B (mucus-secreting cells markers). In accordance with the literature, GLI1 and SHH transcripts were not detected [51,52].

We then confirmed these results by western blot (Fig. 2B). Protein levels of Foxj1 and Gli2 relatively increased over time compared to a basal protein synthesis (Gapdh) (Fig. 2C). In addition, Gli2 detection preceded Foxj1 detection at the protein level confirming transcripts analysis and suggesting an early requirement of HH pathway activation to initiate differentiation. Ck5 and the remaining actors of HH signalling were present throughout the kinetic of differentiation and did not show significant modulation in terms of expression (Fig. 2B and Fig. S1).

Finally, we assessed the cellular localization of the main HH actors on AEC (Fig. 2D). We confirmed previous reports showing the expression of the five proteins Gli1, Gli2, Gli3, Ptch1 and Smo in differentiated AEC (ALI-28), but also demonstrated for the first time their expression in the initial steps of differentiation (ALI-14) [16,24,29,53].

3.2. Shh signalling is crucial for airway multiciliogenesis

Since HH pathway is activated during airway epithelial cells differentiation, we tested whether its alteration may impact the process. To abrogate canonical and non-canonical signalling (ligand-induced) and avoid off-target effects, we used an antibody directed against Shh (AB5E1) in our *in vitro* experiments. Even though it has been already used successfully in the literature to interfere with Shh signalling [39,54,55], we first checked its ability to capture the activator of the pathway in our experimental conditions. One μg/ml of AB5E1 was efficient to deplete free Shh in the medium (Fig. 3A). To fully address the extent of HH pathway inhibition during AEC differentiation, we focused on proliferation, ciliogenesis, mucus production and epithelial barrier integrity (Fig. 3B).

Firstly, we evaluated the proliferative index of AEC to distinguish the process of cell division in regards to proliferation or differentiation. Interestingly, AB5E1 did not influence AEC proliferation before ALI switch (0.86±0.05 vs 0.86±0.04, Fig. S2A and B) but induced a decrease of proliferation in basal cells after ALI switch (65.5 ± 11.6% of Ki67+ cells in CTL vs 38.5 ± 12.5% in AB5E1-treated cells at ALI-14) (Fig. S2C and D) while the proportion of this population remained high instead of progressively reducing as in non-treated cultures (61.6 ± 8.1% of p63+ cells in CTL vs 80.2 ± 6.1% in AB5E1-treated cells) (Fig. 3C and D). Ciliogenesis was also altered with a significant reduction of ciliated cells from ALI-21 (5132.4 ± 1235.3 ciliated cells/mm^2 in CTL vs 2897.7 ± 1879.3 in AB5E1-treated cells) (Fig. S3) that persisted at ALI-28 (1.5-fold decrease) (Fig. 3E and F). Mucous secreting cell fate was not significantly altered considering Muc5ac and Muc5b independently (Fig. S4) but the ratios Muc5ac/Muc5b tended towards an inversion during the course of differentiation (Fig. 3G and H). This is of particular interest when considering that total mucins abundance is altered in COPD patients and the balance between Muc5ac and Muc5b production is essential to warrant optimal muco-ciliary clearance [56–58]. In addition, Muc5ac production is a feature of goblet cells in airways while Muc5b is mainly associated with club-like cells consequently impacting progenitor cell fate is more likely to affect the production of Muc5b than Muc5ac on epithelial cells. Finally, TEER was ultimately reduced (477.8 ± 110.9Ω/cm^2 in CTL vs 314.6 ± 54.8Ω/cm^2 in AB5E1-treated cells) suggesting an alteration of epithelial integrity (Fig. 3I), although no cytoxicity was observed until ALI-35. Altogether, those results indicate that HH pathway inhibition favoured the maintenance of non-differentiated cells while preventing ciliogenesis (Fig. 3J).

We then assessed the molecular mechanisms involved in the alteration of HH pathway. FOXJ1 transcripts were significantly reduced (4.5-fold decrease of FOXJ1 expression at ALI-14) (Fig. 4A) confirming a potential impact on ciliogenesis. MUC5AC and MUC5B transcripts were also significantly reduced at ALI-14 (1.8-fold and 2.8-fold decrease respectively). Regarding to the HH components, GLI2 transcript levels were also reduced upon AB5E1 treatment throughout differentiation (2.1-fold decrease of GLI2 expression at ALI-14) (Fig. 4A). Since the activation of the HH pathway is depicted as a balance between GLI2 and GLI3 [22,59–61], HH pathway inhibition through Gli2 was also confirmed by the reduction of the GLI2/GLI3 ratio from ALI-7 to ALI-35 (Fig. 4B). In addition, Gli2 and Foxj1 protein levels were significantly reduced from ALI-7 in comparison to CTL (Fig. 4C). Furthermore, Gli2 nuclear localization was dramatically reduced upon AB5E1 treatment (Fig. 4D and E) while it was systematically detected in progenitors and ciliated cells (Fig. S5) demonstrating that optimal AEC differentiation required Gli2.

3.3. Shh signalling is altered in COPD patients

Since HH pathway inhibition impacted AEC differentiation *in vitro*, we questioned the *Human Lung Atlas* [62–64] to identify the cell populations where the transcripts of the main actors of the signalling cascade would predominantly be expressed. We confirmed that GLIs, SMO and PTCH1 transcripts were mainly found in progenitors (Fig. 5A and Fig. S6). Because COPD patients were not yet included in the Atlas and large publicly available data sets focused on whole tissue or small airways, we then collected AEC from 10 non-COPD and 10 COPD patients from bronchial brushings of large airways to evaluate HH pathway alteration on a transcriptional level (Table S1). Interestingly, GLI2 transcripts (Fig. 5B) were significantly reduced in COPD AEC (2.3 fold decrease in COPD patients compared to non-COPD) and SMO was not detected (Fig. S7A). Finally, we investigated HH core components localizations in lung tissues obtained from 20 non-COPD and 20 COPD subjects (Table 1).

As recently shown by others, some actors were present in ciliated cells of the airways [29,30] but investigating the five necessary proteins to activate HH targets, we noticed an interesting differential expression between non-COPD and COPD patients on FFPE and frozen lung tissues (Fig. 5C). Strikingly, Gli2 was lost in cilia and nuclei in bronchi (Fig. 5C). Specifically, 66±17.4% of epithelial cells displayed Gli2 in cilia in non-COPD patients compared to 8.9 ± 8.9% in COPD patients, and 87.8 ± 15.1% of epithelial cells presented a nuclear staining of Gli2 in non-COPD patients compared to 37.1 ± 36% in COPD patients (Fig. 5D). We did not observe a significant modification regarding a potential differential localization of Gli1, Gli3 or Ptch1 between non-COPD and COPD patients but the presence of Smo at the cilia and membrane was also affected in COPD patients (Fig. 5C). In particular, Smo localization was lacking in epithelia of patients with COPD: 59.9 ± 25.5% of epithelial cells displayed Smo in cilia in non-COPD patients compared to 5.78±4.8% in COPD patients, and 98±3% of epithelial cells presented membrane-bound Smo in non-COPD patients compared to 32.1 ± 27% in COPD patients (Fig. S7B). In addition, we did not observe any heterogeneity among non-COPD or COPD donors with regard to expression of HH pathway core components.

Because HH pathway activation is mainly appreciated by the addressing of its activating transcription factors to the cell nucleus, we tested the clinical association of nuclear Gli2 in basal AEC with clinical and functional parameters. COPD status was significantly associated with a lower proportion of nuclear Gli2 positive cells (37±1% vs 77±2%). With a retrospective logistic regression, a 25% nuclear Gli2 positive cell threshold allowed to define a significant cut-off, managing to discriminate COPD from non-COPD patients (AUC 0.686, OR=12.833, IC95 =1.738 − 94.784, p = 0.015). Gli2 nuclear positive epithelial cells percentage was further correlated with FEV_1/FVC in a linear regression model (Fig. 5E). Patients with a lower FEV_1/FVC were associated with lower rate of Gli2 nuclear positive epithelial cell. Interestingly, the analysis of Smo localization provided similar conclusions: membrane-bound Smo positive epithelial cells percentage was correlated with FEV_1/FVC in a linear regression model (Fig. S7C).

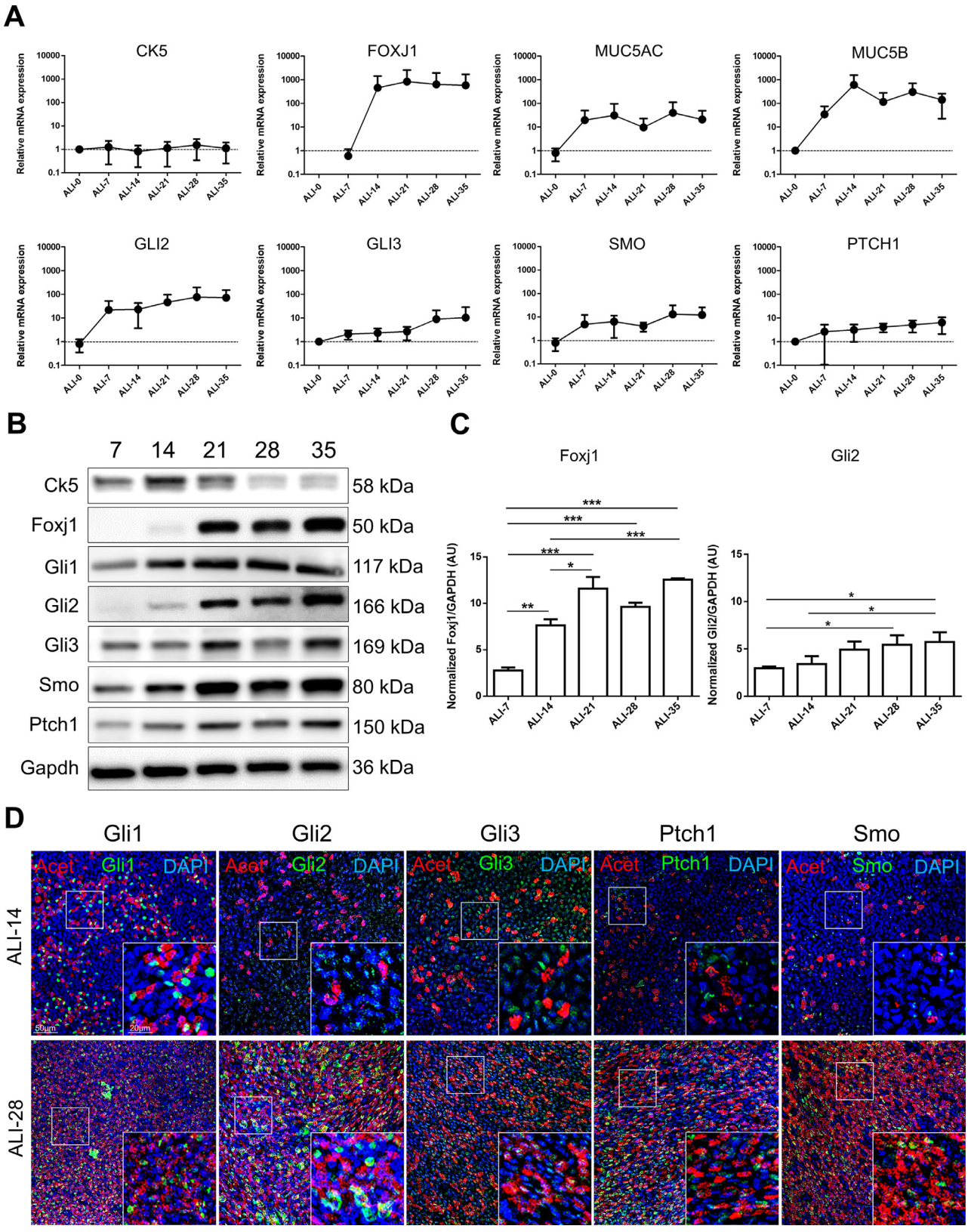

Fig. 2. HH pathway is activated during AEC differentiation. **A**, Curves representing the relative mRNAs levels normalized to GAPDH obtained during the course of ALI cultures by RT-qPCR ($n = 5$) for differentiation markers (CK5, non-differentiated cells; FOXJ1, ciliated cells; and MUC5AC/MUC5B, mucous-secreting cells) and HH pathway elements (GLI2/3; SMO and PTCH1). Means ±SEM of $2^{-\Delta\Delta Ct}$ are shown for each ALI time point. **B**, Representative immunoblots of total proteins extracted from ALI AEC cultures from ALI-7 to ALI-35 for the differentiation markers (Ck5 and Foxj1), HH pathway elements (Gli1/2/3; Smo; Ptch1) and Gapdh ($n = 3$). **C**, Histograms showing the relative increased expressions of Foxj1 and Gli2 protein levels as evaluated by western blot analysis after processing on ImageJ (Gapdh normalized ratios) during the course of AEC differentiation (in arbitrary units, AU). Results show mean ±SEM, $^{*}p < 0.05$, $^{**}p < 0.01$, $^{***}p < 0.001$. **D**, Representative confocal acquisitions from AEC cultures at ALI-14 and ALI-28 for the core HH pathway components Gli1, Gli2, Gli3, Ptch1 and Smo (all green); cilia (acetylated tubulin, red) and cell nuclei (DAPI, blue). Merged z-projections are shown with a magnification corresponding to the selected area.(For interpretation of the references to colour in this figure legend, the reader is referred to the web version of this article.)

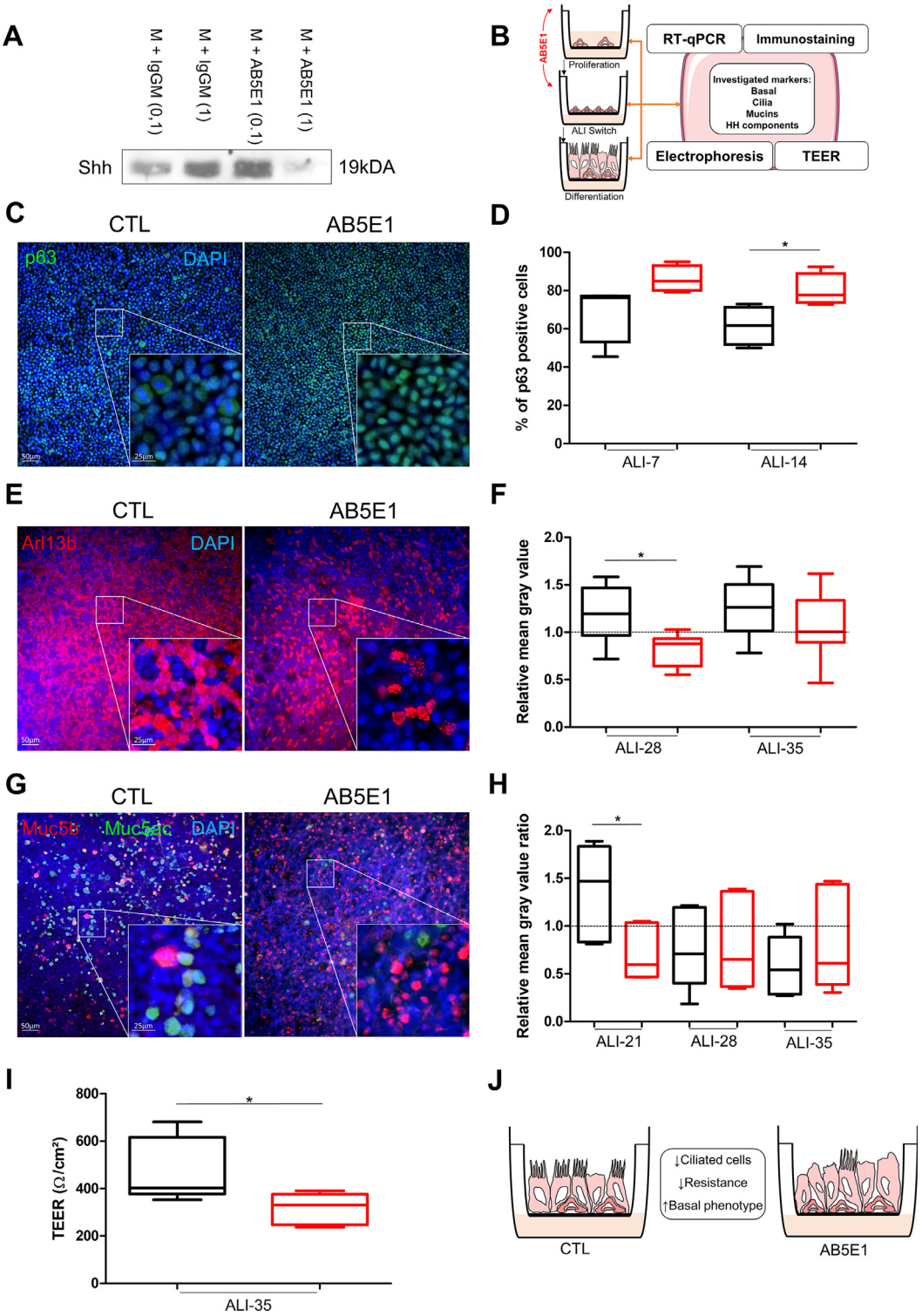

Fig. 3. HH pathway inhibition induced AEC remodelling. **A**, Representative immunoblots from Shh immunoprecipitations in AEC culture medium (n = 3) with control IgGM (0.1 µg/ml and 1 µg/ml) and AB5E1 (0.1 µg/ml and 1 µg/ml). **B**, Schema depicting AEC cultures in the ALI model and AB5E1 treatment in culture medium to investigate transcript levels, protein levels and localizations, and TEER during the process of differentiation. **C**, Examples of micrographs taken from AEC cultures at ALI-14 showing basal cells (p63, green). Nuclei are stained in blue (DAPI). **D**, Box and whiskers plot (median with IQR) represents the percentage of p63+ cells (n = 5) on total cell population (evaluated on DAPI-stained cells count) at ALI-7 and ALI-14 in normal condition (black) and AB5E1-treated cells (red). *$p < 0.05$ CTL vs AB5E1. **E**, Examples of micrographs taken from AEC cultures at ALI-28 showing cilia (Arl13b, red). Nuclei are stained in blue (DAPI). **F**, Box and whiskers plot (median with IQR) represents the relative mean grey values of cilia-associated fluorescence (n = 8) at ALI-28 and ALI-35 (the baseline is given by the average value obtained from ALI-21 in normal condition) in normal condition (black) and AB5E1-treated cells (red). *$p < 0.05$ CTL vs AB5E1. **G**, Examples of micrographs taken from AEC cultures at ALI-21 showing mucins (Muc5b, red; Muc5ac, green). Nuclei are stained in blue (DAPI). **H**, Box and whiskers plot (median with IQR) represents the relative mean grey values of the mucins associated fluorescence ratios Muc5ac/Muc5b (n = 6) at ALI-21, ALI-28 and ALI-35 (the baseline is given by the average value obtained from ALI-14 in normal condition for each mucin) in normal condition (black) and AB5E1-treated cells (red). *$p < 0.05$ CTL vs AB5E1. **I**, Box and whiskers plots (median with IQR) represent the TEER of AEC (n = 5) at ALI-35 in control condition (black) or treated with AB5E1 (red). *$p < 0.05$ CTL vs AB5E1. **J**, Schema summarizing Shh inhibition impact on cell differentiation. (For interpretation of the references to colour in this figure legend, the reader is referred to the web version of this article.)

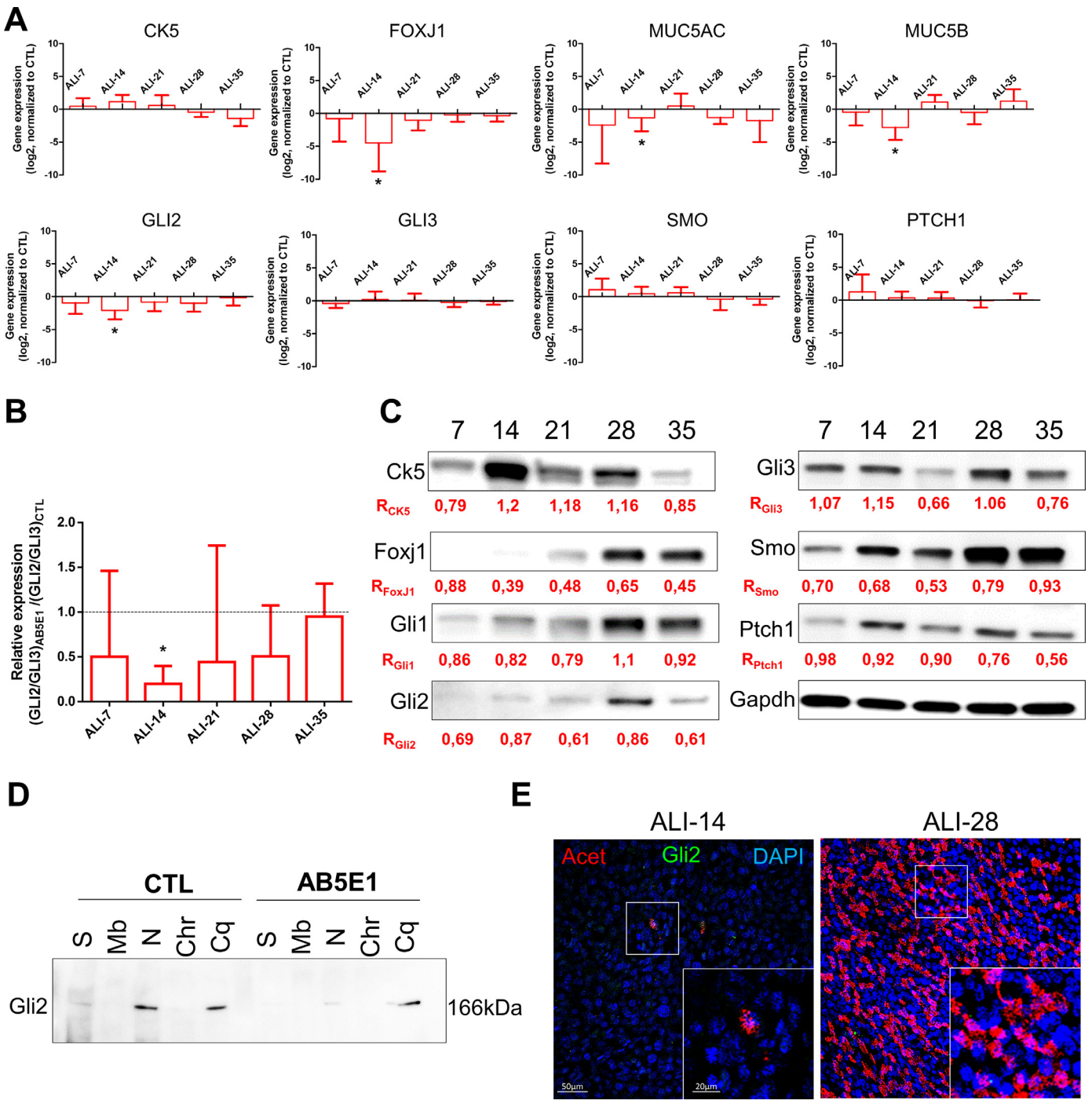

Fig. 4. Shh depletion decreased Gli2 expression and prevented its nuclear translocation. **A**, Histograms representing the assessment of fold-change (log2) in the normalized expression to GAPDH of genes during the course of ALI cultures by RT-qPCR (n = 5) for differentiation markers (CK5, non-differentiated cells; FOXJ1, ciliated cells; and MUC5AC/MUC5B, mucous-secreting cells) and HH pathway elements (GLI2/3; SMO and PTCH1). Results show mean±SEM, $^*p < 0.05$ AB5E1 vs CTL. **B**, Histogram of the ratios of the transcripts levels of GLI2/GLI3 normalized to GAPDH in AB5E1-treated cells in comparison to CTL (median ±SEM are shown). $^*p < 0.05$ AB5E1-treated cells vs CTL. **C**, Representative immunoblots of total proteins extracted from ALI AEC cultures treated with AB5E1 from ALI-0 to ALI-35 for the differentiation markers (Ck5 and Foxj1), HH pathway elements (Gli1/2/3; Smo; Ptch1) and Gapdh (n = 3). Ratios (R) indicate the normalized quantitative analysis of the expression of each protein compared to CTL. **D**, Representative Immunoblot of the fractionated protein extractions on CTL and AB5E1 treated-cells at ALI-7. The fractions are in order: S, soluble proteins; Mb, membrane-bound proteins; N, nuclear proteins; Chr, chromatin-bound proteins; Cq, cytoskeleton-bound proteins. **E**, Representative confocal acquisitions from AEC cultures AB5E1-treated at ALI-14 and ALI-28 for Gli2 (green), cilia (acetylated tubulin, red) and cell nuclei (DAPI, blue). Merged z-projections are shown with a magnification corresponding to the selected area. (For interpretation of the references to colour in this figure legend, the reader is referred to the web version of this article.)

4. Discussion

An outstanding question in respiratory research is what are the molecular actors involved in epithelial remodelling largely responsible for airways obstruction and emphysema. In this study, we identified HH pathway and particularly Gli2 as an essential actor during AEC differentiation and we identified Gli2 and Smo as potential markers of epithelial remodelling in COPD patients.

This report provided the first evidences for the secretion of the ligand Shh by progenitors of airway epithelial cells confirming and supporting previous observations showing Shh localization at the apical side of ciliated AEC on adult lung tissues [29]. To our

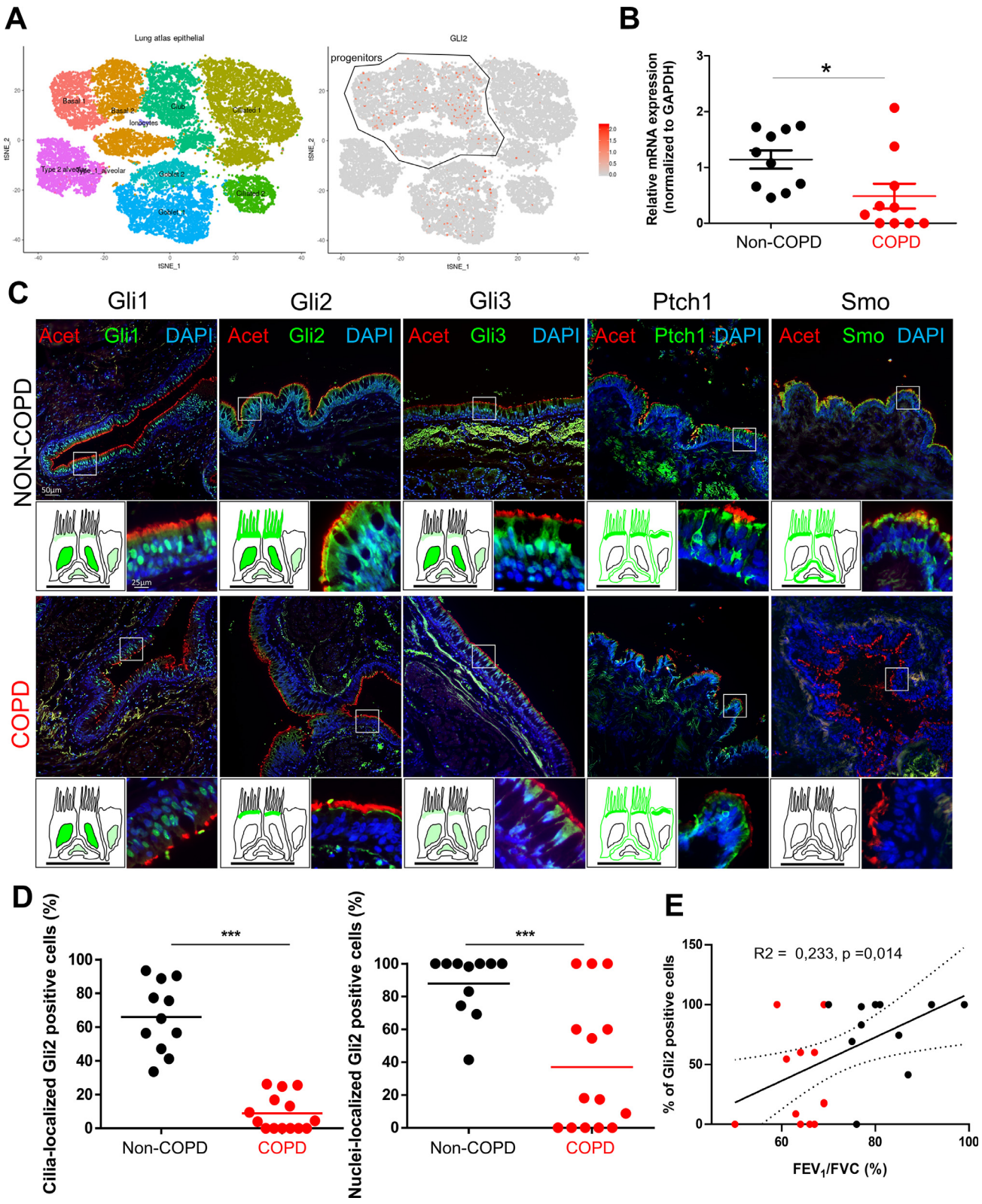

Fig. 5. Alteration of Gli2 localization in AEC is associated with COPD. **A**, Data extracted from the *Human Lung Atlas*. Left, cellular landscape along the airways in human lung analysed by single-cell RNA sequencing from 26154 cells collected from 17 donors to display specific cluster assignment of epithelial cells; right, identification of GLI2-expressing cells by t-distributed Stochastic Neighbour Embedding (tSNE). A progenitor cluster encompassing basal and club-like cells was added. **B**, Dot plot (mean) presenting the relative mRNAs levels normalized to GAPDH obtained on isolated AEC from bronchial brushings by RT-qPCR (n = 20 non-COPD and COPD patients) for GLI2. Means ±SEM of $2^{-\Delta\Delta Ct}$; *$p < 0.05$ non-COPD vs COPD patients. **C**, Representative micrographs showing the bronchi epithelia of non-COPD and COPD patients stained for the core HH pathway components Gli1, Gli2, Gli3, Ptch1 and Smo (all green); cilia (acetylated tubulin, red) and cell nuclei (DAPI, blue). Magnification corresponding to the selected area is shown. Cartoons depict the localization of each HH pathway element (in green). **D**, Dot plots (mean) showing the percentages of Gli2 positive cells in cilia (left panel) and nuclei (right panel) in non-COPD (black) and COPD patients (red). *** $p < 0.001$ non-COPD vs COPD. **E**, Linear regression of the percentages of nuclear Gli2 positive cells according to the FEV_1/FVC (%) for non-COPD (black) and COPD patients (red). (For interpretation of the references to colour in this figure legend, the reader is referred to the web version of this article.)

Table 1
Characteristics of patients (lung tissues).

	Non-COPD (n = 20)	COPD (n = 20)	p
Sex ratio H/F	16/4	18/2	NS
Age, years	68.6 ± 10 [51–86]	66.7 ± 10 [52–84]	NS
Smoking history			
Never smokers	9 (45)	0	< 0.0001*
Current-smokers	4 (20)	13 (65)	0.004*
Former-smokers	7 (35)	7 (35)	NS
Pack-years	16.7 ± 23.4 [0–80]	51 ± 19.3 [20-100]	< 0.0001*
Spirometry			
FEV_1,% of predicted value	97.9 ± 22.6	77.6 ± 16.0	0.003*
FVC,% of predicted value	92.3 ± 21.7	95.2 ± 19.5	NS
FEV_1/FVC%	80.3 ± 7.5	61.5 ± 6.2	< 0.0001*
Spirometric GOLD 1/2/3–4	NA	9/11/0	NS

Data are expressed as mean ± SD or number (%).
FEV_1: Forced Expiratory Volume in one second; FVC: Forced Vital Capacity.
NA: Not applicable, NS: Not significant, *: significant p-value.

knowledge, we assembled for the first time evidence at the level of transcripts, protein expression and localization regarding to the five core elements of the HH pathway (Gli1, Gli2, Gli3, Smo and Ptch1) in the context of airway epithelial cell differentiation and in adult bronchi. We confirmed previous observations of HH pathway actors in ciliated cells but we moved further in the understanding of its role via an *in vitro* experimental approach allowing HH inhibition at the level of the ligand. HH pathway was commonly modulated by pharmacologic inhibitors but their toxicity and off-targets effects were often an issue to interpret results [65–69]. Thus, we resorted to ligand trap with a Shh antibody to abrogate HH activation [39,54]. HH inhibitors are particularly investigated in the context of cancer research because of its overexpression in most of cancers [18,66], and if AB5E1 has not yet reached human trials, it was a strong candidate to safely interfere with HH signalling in a clinical setting [55].

Basal AEC identity and establishment of ciliated cells were particularly impacted upon HH pathway inhibition in the course of *in vitro* differentiation. Evaluating the consequences of AB5E1 presence at the beginning of AEC cultures establishment suggested that HH pathway inhibition was not sufficient to alter proliferation; but epithelial remodelling was observed upon AB5E1 treatment when cells reached confluency to initiate ALI-switch differentiation. Therefore, a distinct role of HH pathway as a driver of non-differentiated cell fate in the context of the lung epithelia was identified. This was in accordance with previous investigations unveiling the importance of HH signalling in regulating the balance between repair and quiescence [24].

The most striking effect of HH pathway inhibition during AEC differentiation was observed on ciliated cells. A strong reduction of cilia was observed from ALI-14 and persisted until ALI-35 although the comparative analysis was not systematically significant. It may be seen as a delay in differentiation related to the availability of the ligand Shh but further molecular characterization will be required to propose a complete mechanical pathway of HH effectors involved in the establishment of a functional epithelium. Alterations of the presence, structure and function of cilia on differentiated AEC were not completely elucidated while the mucociliary clearance was often seen as a readout of normal lung function [70,71]. Mucins secretion was not significantly impacted although there was a trend favouring Muc5b producing cells despite the reduction of MUC5AC and MUC5B transcripts at the beginning of differentiation, therefore it will be interesting to fully characterize cilia and goblet cells alterations upon HH inhibition to understand the molecular events leading to epithelial remodelling particularly since we also observed primary cilia defects in COPD patients [50].

Of particular interest, we unveiled that blocking HH signalling pathway essentially involved Gli2: first, mRNA and protein levels were particularly reduced during the first steps of differentiation indicating that HH pathway inhibition mainly impacted progenitors; second, Gli2 translocation in the nucleus was lost during AEC differentiation. The presence of this transcription factor in nuclei could be used as a tool to evaluate HH pathway activation in homeostasis and pathologic situations. In contrast with a recent report focused on Ptch1 in airways [30], we did not see an overexpression of this receptor in lung tissues but we only included early to moderate COPD patients while the alteration of Ptch1 was shown in moderate to severe COPD tissues. In addition, we performed our immunostaining analysis via immunofluorescence microscopy processing to reduce tissue alteration and we used frozen tissues to better characterize the localization of receptors since FFPE techniques are known to alter membrane-bound proteins [72,73]. The protein levels of Smo were also reduced upon HH inhibition. Interestingly COPD patients were characterized by a strong alteration of this receptor responsible for the binding of the ligand. Thus, the link between these two actors of the signalling cascade will require further evaluation to address the origin of the dysfunction considering the pathway as a whole.

There are four main limitations to this study. Firstly, not all the known elements of HH pathway were investigated. We focused on the three main transcription factors Glis and the two receptors Ptch1 and Smo but of particular interest would be also Suppressor of Fused Homolog (SuFu) which is part of a regulating complex allowing the activation of HH pathway [74]; HH Interacting Protein (HHIP) acting as a ligand receptor and associated with COPD [75–77]; Ptch2, Gas1, Cdo and Boc, all identified as HH receptorsome but not fully characterized in any physiological context [75,78–80]. The second limitation is the experimental approach with AB5E1: maintaining efficient silencing through si/shRNA or selecting clones with CRISPR-Cas9 would improve the robustness of the results but it would be particularly challenging in the context of lung research with primary cells originating from patients where cell differentiation is monitored during several weeks or months [81–83]. Thus we chose to interfere with HH pathway with an antibody directed against the ligand Shh allowing us to act upstream in the signalling cascade and avoiding off-target effects. The third limitation is the source of AEC. Although the primary cells were not directly isolated from bronchi mainly because it did not provide sufficient cells to test all the necessary conditions and collect sufficient materials to analyse, human primary epithelial cells isolated from nasal polyps were a great surrogate to study airway epithelial cell differentiation *in vitro* [13,52,84]. In addition, our data focused on large airways, it would be interesting to repeat the experimental approaches on small airways to complement the observations. The fourth limitation was the source of lung tissues. Patients were all scheduled for lung resection for cancer; we took only in consideration early to moderate COPD patients as we attempted to identify epithelial alterations at the origin of the disease; and finally we focused our observations solely on bronchi to explore potential modifications in the first divisions of the lung airways. Therefore it will be crucial in future research to obtain biological materials devoid of a cancer component and to take into account severe COPD patients and small airways in the analysis.

Our findings highlight the importance of HH signalling in the process of epithelial cell differentiation in the airways. We described Gli2 as a novel important regulator of basal cell fate to emphasize the utmost significance of understanding progenitor cell homeostasis [85]. In addition, we provided the first analysis of HH pathway core components in COPD. Evaluation of Gli2 localization in airways may provide a useful tool to characterize COPD patients and help designing innovative therapeutics to oppose epithelial remodelling and thus improve respiratory functions.

Declaration of competing interest

Dr. Deslee reports personal fees from Nuvaira, personal fees from BTG/PneumRx, personal fees from Chiesi, personal fees from Boehringer, personal fees from Astra Zeneca, outside the submitted work.

Acknowledgments

We thank the members of the Inserm UMR-S 1250 unit and our collaborators for their helpful comments and insights. We thank the Platform of Cell and Tissue Imaging (PICT) for technical assistance. We thank Clinic *La Sagesse* for their collaboration in sample collection.

Funding sources

This work was supported by Funding from University of Reims Champagne-Ardenne (URCA) and the French National Institute of Health and Medical Research (Inserm). It was carried out in the framework of the Federative Research Structure *CAP-Santé* and benefited from the Project Research and Innovation in Inflammatory Respiratory Diseases (RINNOPARI).

Author contributions

RB, MP, GaD and VD designed the research. JA, JMP, PB, XD, JCM, GoD and GaD provided the human samples and clinical characterization. RB, EL, ZD, AG, NL and VD performed experiments. RB, JA, JMP, PB, GaD and VD analysed data. RB, JA, GaD and VD wrote the paper. All authors approved the submitted version of the manuscript.

Supplementary materials

Supplementary material associated with this article can be found in the online version at doi:10.1016/j.ebiom.2019.11.033.

References

[1] Criner RN, Han MK. COPD care in the 21st century: a public health priority. Respir Care 2018;63:591–600. doi: 10.4187/respcare.06276.
[2] Miravitlles M, Roche N, Cardoso J, Halpin D, Aisanov Z, Kankaanranta H, et al. Chronic obstructive pulmonary disease guidelines in Europe: a look into the future. Respir Res 2018;19:11. doi: 10.1186/s12931-018-0715-1.
[3] Singh D, Agusti A, Anzueto A, Barnes PJ, Bourbeau J, Celli BR, et al. Global strategy for the diagnosis, management, and prevention of chronic obstructive lung disease: the gold science committee report 2019. Eur Respirat J 2019:1900164. doi: 10.1183/13993003.00164-2019.
[4] Hangaard S, Helle T, Nielsen C, Hejlesen OK. Causes of misdiagnosis of chronic obstructive pulmonary disease: a systematic scoping review. Respir Med 2017;129:63–84. doi: 10.1016/j.rmed.2017.05.015.
[5] Stockley JA, Cooper BG, Stockley RA, Sapey E. Small airways disease: time for a revisit? Int J Chron Obstruct Pulmon Dis 2017;12:2343–53. doi: 10.2147/COPD.S138540.
[6] Roche N. Stable COPD treatment: where are we? COPD 2018;15:123–9. doi: 10.1080/15412555.2018.1445214.
[7] Wechsler ME. Current and emerging biologic therapies for asthma and COPD. Respir Care 2018;63:699–707. doi: 10.4187/respcare.06322.
[8] Riley CM, Sciurba FC. Diagnosis and outpatient management of chronic obstructive pulmonary disease: a review. JAMA 2019;321:786–97. doi: 10.1001/jama.2019.0131.
[9] Hirota N, Martin JG. Mechanisms of airway remodeling. Chest 2013;144:1026–32. doi: 10.1378/chest.12-3073.
[10] Higham A, Quinn AM, Cançado JED, Singh D. The pathology of small airways disease in COPD: historical aspects and future directions. Respir Res 2019;20:49. doi: 10.1186/s12931-019-1017-y.
[11] Sohal SS. Epithelial and endothelial cell plasticity in chronic obstructive pulmonary disease (COPD). Respir Investig 2017;55:104–13. doi: 10.1016/j.resinv.2016.11.006.
[12] Tilley AE, Walters MS, Shaykhiev R, Crystal RG. Cilia dysfunction in lung disease. Annu Rev Physiol 2015;77:379–406. doi: 10.1146/annurev-physiol-021014-071931.
[13] Yaghi A, Zaman A, Cox G, Dolovich MB. Ciliary beating is depressed in nasal cilia from chronic obstructive pulmonary disease subjects. Respir Med 2012;106:1139–47. doi: 10.1016/j.rmed.2012.04.001.
[14] Zuo W-L, Yang J, Strulovici-Barel Y, Salit J, Rostami M, Mezey JG, et al. Exaggerated BMP4 signalling alters human airway basal progenitor cell differentiation to cigarette smoking-related phenotypes. Eur Respir J 2019;53. doi: 10.1183/13993003.02553-2017.
[15] Kugler MC, Joyner AL, Loomis CA, Munger JS. Sonic hedgehog signaling in the lung from development to disease. Am J Respir Cell Mol Biol 2015;52:1–13. doi: 10.1165/rcmb.2014-0132TR.
[16] Bolaños AL, Milla CM, Lira JC, Ramírez R, Checa M, Barrera L, et al. Role of sonic Hedgehog in idiopathic pulmonary fibrosis. Am J Physiol Lung Cell Mol Physiol 2012;303:L978–90. doi: 10.1152/ajplung.00184.2012.
[17] Wang C, de Mochel NSR, Christenson SA, Cassandras M, Moon R, Brumwell AN, et al. Expansion of hedgehog disrupts mesenchymal identity and induces emphysema phenotype. J Clin Invest 2018;128:4343–58. doi: 10.1172/JCI99435.
[18] Carballo GB, Honorato JR, de Lopes GPF, Spohr TCL, de SE. A highlight on sonic hedgehog pathway. Cell Commun Signal 2018;16:11. doi: 10.1186/s12964-018-0220-7.
[19] Kong JH, Siebold C, Rohatgi R. Biochemical mechanisms of vertebrate hedgehog signaling. Development 2019;146. doi: 10.1242/dev.166892.
[20] Regan JL, Schumacher D, Staudte S, Steffen A, Haybaeck J, Keilholz U, et al. Non-canonical hedgehog signaling is a positive regulator of the WNT pathway and is required for the survival of colon cancer stem cells. Cell Rep 2017;21:2813–28. doi: 10.1016/j.celrep.2017.11.025.
[21] Brennan D, Chen X, Cheng L, Mahoney M, Riobo NA. Noncanonical Hedgehog signaling. Vitam Horm 2012;88:55–72. doi: 10.1016/B978-0-12-394622-5.00003-1.
[22] Fernandes-Silva H, Correia-Pinto J, Moura RS. Canonical sonic hedgehog signaling in early lung development. J Dev Biol 2017;5. doi: 10.3390/jdb5010003.
[23] Kugler MC, Loomis CA, Zhao Z, Cushman JC, Liu L, Munger JS. Sonic hedgehog signaling regulates myofibroblast function during alveolar septum formation in murine postnatal lung. Am J Respir Cell Mol Biol 2017;57:280–93. doi: 10.1165/rcmb.2016-0268OC.
[24] Peng T, Frank DB, Kadzik RS, Morley MP, Rathi KS, Wang T, et al. Hedgehog actively maintains adult lung quiescence and regulates repair and regeneration. Nature 2015;526:578–82. doi: 10.1038/nature14984.
[25] Sriperumbudur A, Breitzig M, Lockey R, Kolliputi N. Hedgehog: the key to maintaining adult lung repair and regeneration. J Cell Commun Signal 2017;11:95–6. doi: 10.1007/s12079-016-0365-3.
[26] Pillai SG, Ge D, Zhu G, Kong X, Shianna KV, Need AC, et al. A genome-wide association study in chronic obstructive pulmonary disease (COPD): identification of two major susceptibility loci. PLoS Genet 2009;5:e1000421. doi: 10.1371/journal.pgen.1000421.
[27] Kim WJ, Lee SD. Candidate genes for COPD: current evidence and research. Int J Chron Obstruct Pulmon Dis 2015;10:2249–55. doi: 10.2147/COPD.S80227.
[28] Li Y, Cho MH, Zhou X. What do polymorphisms tell us about the mechanisms of COPD? Clin Sci 2017;131:2847–63. doi: 10.1042/CS20160718.
[29] Mao S, Shah AS, Moninger TO, Ostedgaard LS, Lu L, Tang XX, et al. Motile cilia of human airway epithelia contain hedgehog signaling components that mediate noncanonical hedgehog signaling. Proc Natl Acad Sci USA 2018;115:1370–5. doi: 10.1073/pnas.1719177115.
[30] Tam A, Hughes M, McNagny KM, Obeidat M, Hackett TL, Leung JM, et al. Hedgehog signaling in the airway epithelium of patients with chronic obstructive pulmonary disease. Sci Rep 2019;9:3353. doi: 10.1038/s41598-019-40045-3.
[31] Du Rand IA, Blaikley J, Booton R, Chaudhuri N, Gupta V, Khalid S, et al. British thoracic society guideline for diagnostic flexible bronchoscopy in adults: accredited by nice. Thorax 2013;68:i1–44. doi: 10.1136/thoraxjnl-2013-203618.
[32] Ho T, Cusack RP, Chaudhary N, Satia I, Kurmi OP. Under- and over-diagnosis of COPD: a global perspective. Breathe (Sheff) 2019;15:24–35. doi: 10.1183/20734735.0346-2018.
[33] Adam D, Roux-Delrieu J, Luczka E, Bonnomet A, Lesage J, Mérol J-C, et al. Cystic fibrosis airway epithelium remodelling: involvement of inflammation. J Pathol 2015;235:408–19. doi: 10.1002/path.4471.
[34] Jiang D, Schaefer N, Chu HW. Air-liquid interface culture of human and mouse airway epithelial cells. Methods Mol Biol 2018;1809:91–109. doi: 10.1007/978-1-4939-8570-8_8.
[35] Schamberger AC, Staab-Weijnitz CA, Mise-Racek N, Eickelberg O. Cigarette smoke alters primary human bronchial epithelial cell differentiation at the air-liquid interface. Sci Rep 2015;5:8163. doi: 10.1038/srep08163.
[36] Müller L, Brighton LE, Carson JL, Fischer WA, Jaspers I. Culturing of human nasal epithelial cells at the air liquid interface. J Vis Exp 2013. doi: 10.3791/50646.
[37] Pezzulo AA, Starner TD, Scheetz TE, Traver GL, Tilley AE, Harvey B-G, et al. The air-liquid interface and use of primary cell cultures are important to recapitulate the transcriptional profile of in vivo airway epithelia. Am J Physiol Lung Cell Mol Physiol 2011;300:L25–31. doi: 10.1152/ajplung.00256.2010.
[38] Ruiz García S, Deprez M, Lebrigand K, Cavard A, Paquet A, Arguel M-J, et al. Novel dynamics of human mucociliary differentiation revealed by single-cell RNA sequencing of nasal epithelial cultures. Development 2019. doi: 10.1242/dev.177428.
[39] Maun HR, Wen X, Lingel A, de Sauvage FJ, Lazarus RA, Scales SJ, et al. Hedgehog pathway antagonist 5E1 binds hedgehog at the pseudo-active site. J Biol Chem 2010;285:26570–80. doi: 10.1074/jbc.M110.112284.
[40] Ericson J, Morton S, Kawakami A, Roelink H, Jessell TM. Two critical periods of sonic hedgehog signaling required for the specification of motor neuron identity. Cell 1996;87:661–73. doi: 10.1016/s0092-8674(00)81386-0.
[41] Wang LC, Liu ZY, Gambardella L, Delacour A, Shapiro R, Yang J, et al. Regular articles: conditional disruption of hedgehog signaling pathway defines its critical role in hair development and regeneration. J Invest Dermatol 2000;114:901–8. doi: 10.1046/j.1523-1747.2000.00951.x.
[42] Pepinsky RB, Rayhorn P, Day ES, Dergay A, Williams KP, Galdes A, et al. Mapping sonic hedgehog-receptor interactions by steric interference. J Biol Chem 2000;275:10995–1001. doi: 10.1074/jbc.275.15.10995.

[43] Pepinsky RB, Zeng C, Wen D, Rayhorn P, Baker DP, Williams KP, et al. Identification of a palmitic acid-modified form of human sonic hedgehog. J Biol Chem 1998;273:14037–45. doi: 10.1074/jbc.273.22.14037.
[44] Chaudary N, Pintilie M, Hedley D, Hill RP, Milosevic M, Mackay H. Hedgehog inhibition enhances efficacy of radiation and cisplatin in orthotopic cervical cancer xenografts. Br J Cancer 2017;116:50–7. doi: 10.1038/bjc.2016.383.
[45] Donnelly JM, Chawla A, Houghton J, Zavros Y. Sonic hedgehog mediates the proliferation and recruitment of transformed mesenchymal stem cells to the stomach. PLoS One 2013;8:e75225. doi: 10.1371/journal.pone.0075225.
[46] Alfaro AC, Roberts B, Kwong L, Bijlsma MF, Roelink H. Ptch2 mediates the Shh response in Ptch1-/- cells. Development 2014;141:3331–9. doi: 10.1242/dev.110056.
[47] Xiao C, Ogle SA, Schumacher MA, Schilling N, Tokhunts RA, Orr-Asman MA, et al. Hedgehog signaling regulates E-cadherin expression for the maintenance of the actin cytoskeleton and tight junctions. Am J Physiol Gastrointest Liver Physiol 2010;299:G1252–65. doi: 10.1152/ajpgi.00512.2009.
[48] Bailey JM, Swanson BJ, Hamada T, Eggers JP, Singh PK, Caffery T, et al. Sonic hedgehog promotes desmoplasia in pancreatic cancer. Clin Cancer Res 2008;14:5995–6004. doi: 10.1158/1078-0432.CCR-08-0291.
[49] Pascual O, Traiffort E, Baker DP, Galdes A, Ruat M, Champagnat J. Sonic hedgehog signalling in neurons of adult ventrolateral nucleus tractus solitarius. Eur J Neurosci 2005;22:389–96. doi: 10.1111/j.1460-9568.2005.04223.x.
[50] Perotin J-M, Coraux C, Lagonotte E, Birembaut P, Delepine G, Polette M, et al. Alteration of primary cilia in COPD. Eur Respir J 2018;52. doi: 10.1183/13993003.00122-2018.
[51] Katoh Y, Katoh M. Integrative genomic analyses on GLI1: positive regulation of GLI1 by Hedgehog-GLI, TGFbeta-Smads, and RTK-PI3K-AKT signals, and negative regulation of GLI1 by Notch-CSL-HES/HEY, and GPCR-Gs-PKA signals. Int J Oncol 2009;35:187–92. doi: 10.3892/ijo_00000328.
[52] Giovannini-Chami L, Paquet A, Sanfiorenzo C, Pons N, Cazareth J, Magnone V, et al. The “one airway, one disease” concept in light of Th2 inflammation. Eur Respir J 2018;52. doi: 10.1183/13993003.00437-2018.
[53] Cigna N, Farrokhi Moshai E, Brayer S, Marchal-Somme J, Wémeau-Stervinou L, Fabre A, et al. The hedgehog system machinery controls transforming growth factor-β-dependent myofibroblastic differentiation in humans: involvement in idiopathic pulmonary fibrosis. Am J Pathol 2012;181:2126–37. doi: 10.1016/j.ajpath.2012.08.019.
[54] Kugler MC, Yie T-A, Cai Y, Berger JZ, Loomis CA, Munger JS. The Hedgehog target GLI1 is not required for bleomycin-induced lung fibrosis. Exp Lung Res 2019;45:22–9. doi: 10.1080/01902148.2019.1601795.
[55] Rimkus TK, Carpenter RL, Qasem S, Chan M, Lo H-W. Targeting the sonic hedgehog signaling pathway: review of smoothened and GLI inhibitors. Cancers (Basel) 2016;8. doi: 10.3390/cancers8020022.
[56] Kesimer M, Ford AA, Ceppe A, Radicioni G, Cao R, Davis CW, et al. Airway mucin concentration as a marker of chronic bronchitis. N Engl J Med 2017;377:911–22. doi: 10.1056/NEJMoa1701632.
[57] Ma J, Rubin BK, Voynow JA. Mucins, mucus, and goblet cells. Chest 2018;154:169–76. doi: 10.1016/j.chest.2017.11.008.
[58] Ostedgaard LS, Moninger TO, McMenimen JD, Sawin NM, Parker CP, Thornell IM, et al. Gel-forming mucins form distinct morphologic structures in airways. Proc Natl Acad Sci USA 2017;114:6842–7. doi: 10.1073/pnas.1703228114.
[59] Wu F, Zhang Y, Sun B, McMahon AP, Wang Y. Hedgehog signaling: from basic biology to cancer therapy. Cell Chem Biol 2017;24:252–80. doi: 10.1016/j.chembiol.2017.02.010.
[60] Falkenstein KN, Vokes SA. Transcriptional regulation of graded Hedgehog signaling. Semin Cell Dev Biol 2014;33:73–80. doi: 10.1016/j.semcdb.2014.05.010.
[61] Niewiadomski P, Niedziółka SM, Markiewicz Ł, Uśpieński T, Baran B, Chojnowska K. Gli proteins: regulation in development and cancer. Cells 2019;8. doi: 10.3390/cells8020147.
[62] Schiller HB, Montoro DT, Simon LM, Rawlins EL, Meyer KB, Strunz M, et al. The human lung cell atlas: a high-resolution reference map of the human lung in health and disease. Am J Respir Cell Mol Biol 2019;61:31–41. doi: 10.1165/rcmb.2018-0416TR.
[63] Reyfman PA, Walter JM, Joshi N, Anekalla KR, McQuattie-Pimentel AC, Chiu S, et al. Single-cell transcriptomic analysis of human lung provides insights into the pathobiology of pulmonary fibrosis. Am J Respir Crit Care Med 2019;199:1517–36. doi: 10.1164/rccm.201712-2410OC.
[64] Ordovas-Montanes J, Dwyer DF, Nyquist SK, Buchheit KM, Vukovic M, Deb C, et al. Allergic inflammatory memory in human respiratory epithelial progenitor cells. Nature 2018;560:649–54. doi: 10.1038/s41586-018-0449-8.
[65] Peer E, Tesanovic S, Aberger F. Next-generation Hedgehog/GLI pathway inhibitors for cancer therapy. Cancers (Basel) 2019;11. doi: 10.3390/cancers11040538.
[66] Xie H, Paradise BD, Ma WW, Fernandez-Zapico ME. Recent advances in the clinical targeting of Hedgehog/GLI signaling in cancer. Cells 2019;8. doi: 10.3390/cells8050394.
[67] Girardi D, Barrichello A, Fernandes G, Pereira A. Targeting the Hedgehog pathway in cancer: current evidence and future perspectives. Cells 2019;8. doi: 10.3390/cells8020153.
[68] Salaritabar A, Berindan-Neagoe I, Darvish B, Hadjiakhoondi F, Manayi A, Devi KP, et al. Targeting Hedgehog signaling pathway: paving the road for cancer therapy. Pharmacol Res 2019;141:466–80. doi: 10.1016/j.phrs.2019.01.014.
[69] Sabol M, Trnski D, Musani V, Ozretić P, Levanat S. Role of GLI transcription factors in pathogenesis and their potential as new therapeutic targets. Int J Mol Sci 2018;19. doi: 10.3390/ijms19092562.
[70] Bustamante-Marin XM, Ostrowski LE. Cilia and mucociliary clearance. Cold Spring Harb Perspect Biol 2017;9:a028241. doi: 10.1101/cshperspect.a028241.
[71] Whitsett JA. Airway epithelial differentiation and mucociliary clearance. Ann Am Thorac Soc 2018;15:S143–8. doi: 10.1513/AnnalsATS.201802-128AW.
[72] Magaki S, Hojat SA, Wei B, So A, Yong WH. An introduction to the performance of immunohistochemistry. Methods Mol Biol 2019;1897:289–98. doi: 10.1007/978-1-4939-8935-5_25.
[73] Gandjeva A, Tuder RM. Lung histological methods. Methods Mol Biol 2018;1809:315–29. doi: 10.1007/978-1-4939-8570-8_20.
[74] Huang D, Wang Y, Tang J, Luo S. Molecular mechanisms of suppressor of fused in regulating the hedgehog signalling pathway. Oncol Lett 2018;15:6077–86. doi: 10.3892/ol.2018.8142.
[75] Holtz AM, Peterson KA, Nishi Y, Morin S, Song JY, Charron F, et al. Essential role for ligand-dependent feedback antagonism of vertebrate hedgehog signaling by PTCH1, PTCH2 and HHIP1 during neural patterning. Development 2013;140:3423–34. doi: 10.1242/dev.095083.
[76] Prokopenko D, Sakornsakolpat P, Fier HL, Qiao D, Parker MM, McDonald M-LN, et al. Whole-Genome sequencing in severe chronic obstructive pulmonary disease. Am J Respir Cell Mol Biol 2018;59:614–22. doi: 10.1165/rcmb.2018-0088OC.
[77] Wan ES, Li Y, Lao T, Qiu W, Jiang Z, Mancini JD, et al. Metabolomic profiling in a hedgehog interacting protein (Hhip) murine model of chronic obstructive pulmonary disease. Sci Rep 2017;7:2504. doi: 10.1038/s41598-017-02701-4.
[78] Jeong M-H, Leem Y-E, Kim H-J, Kang K, Cho H, Kang J-S. A Shh coreceptor Cdo is required for efficient cardiomyogenesis of pluripotent stem cells. J Mol Cell Cardiol 2016;93:57–66. doi: 10.1016/j.yjmcc.2016.01.013.
[79] Jin S, Martinelli DC, Zheng X, Tessier-Lavigne M, Fan C-M. Gas1 is a receptor for sonic hedgehog to repel enteric axons. Proc Natl Acad Sci USA 2015;112:E73–80. doi: 10.1073/pnas.1418629112.
[80] Izzi L, Lévesque M, Morin S, Laniel D, Wilkes BC, Mille F, et al. Boc and Gas1 each form distinct Shh receptor complexes with Ptch1 and are required for Shh-mediated cell proliferation. Dev Cell 2011;20:788–801. doi: 10.1016/j.devcel.2011.04.017.
[81] Alapati D, Morrisey EE. Gene editing and genetic lung disease. basic research meets therapeutic application. Am J Respir Cell Mol Biol 2017;56:283–90. doi: 10.1165/rcmb.2016-0301PS.
[82] Dakhama A, Chu HW. The use of CRISPR-Cas9 technology to reveal important aspects of human airway biology. Methods Mol Biol 2018;1799:371–80. doi: 10.1007/978-1-4939-7896-0_27.
[83] Rosen BH, Chanson M, Gawenis LR, Liu J, Sofoluwe A, Zoso A, et al. Animal and model systems for studying cystic fibrosis. J Cyst Fibros 2018;17:S28–34. doi: 10.1016/j.jcf.2017.09.001.
[84] Brewington JJ, Filbrandt ET, LaRosa FJ, Moncivaiz JD, Ostmann AJ, Strecker LM, et al. Brushed nasal epithelial cells are a surrogate for bronchial epithelial CFTR studies. JCI Insight 2018;3. doi: 10.1172/jci.insight.99385.
[85] Crystal RG. Airway basal cells. The “smoking gun” of chronic obstructive pulmonary disease. Am J Respir Crit Care Med 2014;190:1355–62. doi: 10.1164/rccm.201408-1492PP.